Original Article

Quantitative parameters of diffusion tensor imaging in the evaluation of carpal tunnel syndrome

Nhu Quynh Vo[1]^, Ngoc Thanh Hoang[1]^, Duy Duan Nguyen[2]^, Thi Hieu Dung Nguyen[3], Trong Binh Le[1]^, Nghi Thanh Nhan Le[4], Thanh Thao Nguyen[1]^

[1]Department of Radiology, University of Medicine and Pharmacy, Hue University, Hue, Vietnam; [2]Department of Internal Medicine, University of Medicine and Pharmacy, Hue University, Hue, Vietnam; [3]Department of Physiology, University of Medicine and Pharmacy, Hue University, Hue, Vietnam; [4]Department of Surgery, University of Medicine and Pharmacy, Hue University, Hue, Vietnam

Contributions: (I) Conception and design: TT Nguyen; (II) Administrative support: NT Hoang; (III) Provision of study materials or patients: NT Hoang, DD Nguyen, THD Nguyen; (IV) Collection and assembly of data: NQ Vo, TT Nguyen; (V) Data analysis and interpretation: TT Nguyen, NQ Vo, NTN Le; (VI) Manuscript writing: All authors; (VII) Final approval of manuscript: All authors.

Correspondence to: Thanh Thao Nguyen. Department of Radiology, University of Medicine and Pharmacy, Hue University, 6 Ngo Quyen Street, Hue 53000, Vietnam. Email: ntthao@hueuni.edu.vn.

Background: To explore the value of diffusion tensor imaging (DTI)-derived metrics in quantitative evaluation of carpal tunnel syndrome (CTS).

Methods: This prospective cross-sectional study included 39 wrists from 24 symptomatic CTS patients, who underwent clinical, electrophysiological, and magnetic resonance imaging (MRI) evaluations. In addition, 10 wrists of 6 healthy participants were included as controls. Clinical and nerve conduction study (NCS) findings were evaluated and graded according to the Boston Carpal Tunnel Questionnaire (BCTQ) and the American Association of Neuromuscular and Electrodiagnostic Medicine (AANEM), respectively. We performed MRI using a 1.5 Tesla scanner. Mean diffusivity (MD), fractional anisotropy (FA), axial diffusivity (AD), and radial diffusivity (RD) of the median nerve at the distal radioulnar joint (DRUJ) (d), the inlet of the carpal tunnel (CT) at the pisiform level (i), the middle of the CT (m) and the outlet of the CT at the level of the hook of hamate (o), cross-sectional area at the inlet of the CT (iCSA), and the difference between MD and FA of the DRUJ and the outlet of CT (Delta MD and Delta FA) were measured.

Results: The CTS patients had significantly lower FA [for example, oFA: mean difference 0.09, 95% confidence interval (CI): 0.05 to 0.12] and significantly higher MD than healthy participants (for example, iMD: mean difference 0.3, 95% CI: 0.03 to 0.57). There was a negative correlation between iCSA with iFA and between mFA and oFA ($-0.5<R<-0.4$). There was a positive correlation between distal motor latency time and Delta MD ($R=0.57$) and a negative correlation between distal motor latency time and Delta FA ($R=-0.51$). The FA demonstrated a somewhat strong negative correlation with the Boston scores for symptom and function.

Conclusions: The DTI-derived quantitative metrics add potential value to the evaluation of CTS. Alterations in the FA of the median nerve along the CT are the most significant features of CTS and reflect the degree of median nerve compression and clinical deficit. With a cutoff value of 0.45, FA at the carpal outlet has a sensitivity and specificity of 87.5% and 85.7% in the diagnosis of CTS, respectively.

Keywords: Carpal tunnel syndrome (CTS); magnetic resonance imaging (MRI); diffusion tensor imaging (DTI); fraction anisotropy; apparent diffusion coefficient (ADC); Boston Carpal Tunnel Questionnaire; nerve conduction study (NCS)

^ ORCID: Thanh Thao Nguyen, 0000-0001-9379-6359; Nhu Quynh Vo, 0000-0002-4851-6079; Ngoc Thanh Hoang, 0000-0002-9498-464X; Duy Duan Nguyen, 0000-0002-4773-1471; Trong Binh Le, 0000-0001-5444-5708.

© Quantitative Imaging in Medicine and Surgery. All rights reserved.

Submitted Sep 10, 2021. Accepted for publication Mar 16, 2022.
doi: 10.21037/qims-21-910
View this article at: https://dx.doi.org/10.21037/qims-21-910

Introduction

Diffusion tensor imaging (DTI) is a noninvasive magnetic resonance imaging (MRI) technique to measure the diffusion of water within biological tissues (1). It has been used to identify microstructural changes in tissues via alterations in quantitative parameters (2-6). The most common DTI-derived metrics are mean diffusivity (MD), fractional anisotropy (FA), axial diffusivity (AD), and radial diffusivity (RD). Numerous studies have successfully used DTI to explore peripheral nerves, including the median nerve in carpal tunnel syndrome (CTS) (7-11).

In CTS, the median nerve is compressed within the carpal tunnel (CT) at the wrist level (12). It is the most common peripheral nerve entrapment syndrome (13,14). The diagnosis of CTS is made based on medical history, clinical tests, and nerve conduction study (NCS) (12,15). Imaging modalities, including ultrasound and MRI, are increasingly being used as diagnostic tools in evaluating CTS, especially to rule out potential causes of secondary CTS (16-18). In addition to ultrasound, MRI has the advantages of providing valuable information on CT anatomy in an objective and unbiased way. While conventional MRI provides only qualitative information, DTI allows quantitative evaluation of the microstructure through alterations in water diffusion (19). The metrics of MD and FA present the degree and the anisotropic nature of water molecules diffusion within tissues; AD can reflect axon integrity, while changes in RD and FA may indicate myelin sheath injury (20). In published studies, the diagnostic capacity of DTI was compared with those of conventional MRI and NCS to determine the role of DTI in the diagnosis of CTS (8-11). The DTI-derived metrics have been found to have potential value in the diagnosis of idiopathic CTS (10,21,22). In this study, we aimed to explore the value of DTI-derived metrics in quantitatively evaluating CTS.

We present the following article in accordance with the Strengthening the Reporting of Observational Studies in Epidemiology (STROBE) reporting checklist (available at https://qims.amegroups.com/article/view/10.21037/qims-21-910/rc).

Methods

Patients diagnosed with CTS at Hue University of Medicine and Pharmacy Hospital between April 2020 and August 2021 were included in this study. This prospective cross-sectional study was conducted in accordance with the Declaration of Helsinki (as revised in 2013). The study was approved by the Ethics Committee of the University of Medicine and Pharmacy, Hue University, Vietnam (No. H2020/159). All participants provided their written informed consent. The reporting of this study conforms to the STROBE guidelines (23). The inclusion criteria were clinical and NCS findings according to the American Academy of Neurology (24). The exclusion criteria were general contraindications for MRI, a prior history of surgery or trauma of the wrist, and predisposing factors for secondary CTS, such as those with diabetes mellitus, gout, and inflammatory arthropathy diseases (17). Age-matched healthy participants without clinical symptoms or a history of neurological symptoms were randomly selected and included for control purposes.

Clinical and electrophysiological study

The diagnostic criteria for CTS according to the American Academy of Neurology include at least 1 clinical sign and evidence of median nerve impairment through the CT on electrophysiology, while other nerves are normal (25). Participants were clinically evaluated using the Boston Carpal Tunnel questionnaire (BCTQ), including the functional and symptom Boston scores (26), followed by NCS. The CTS of patients was classified into mild, moderate, and severe stages based on NCS findings (electrophysiological stages) as described by Steven *et al.* (27).

The BCTQ includes 11 symptom questions and 8 function questions. The symptom severity scale is categorized as asymptomatic, mild, moderate, severe, and very severe. Functional status was staged as no difficulty or mild, moderate, intense, or very severe difficulty (cannot perform the activity at all due to hand and wrist symptoms). Based on the mean value of each score, symptom severity and functional status were graded as follows: normal: =1;

© Quantitative Imaging in Medicine and Surgery. All rights reserved.

mild: ≤2, moderate: ≤3, severe ≤4, and very severe: ≤5 (26).

MRI technique

The MRI scans were performed using a 1.5 T MRI system (Siemens Magnetom Amira, Erlangen, Germany) and a standard 16-channel wrist coil. All participants were scanned 'feet first' in a supine neutral position, with palms facing the body, all fingers straightened, and thumbs pointing upwards. The imaging protocol included a single-shot echo planar imaging sequence with the following imaging parameters: repetition time (TR) 4,000 ms, echo time (TE) 95 ms, b-factor (s/mm^2) and averages (0, 800 and 4, respectively), 30 slices of 2.5 mm thickness with no gap in between, bandwidth of 1,100 with a field of view (FOV) of 16×16 cm, matrix size of 64×64 (in-plane resolution of 2.5×2.5 mm^2), acceleration factors of 2 (GRAPPA), 30 diffusion directions, voxel-size 2.5×2.5×2.5 mm^3, and scan duration 8.28 minutes. Conventional MRI sequences, including T1-weighted (T1W) axial with the following parameters: TR =500 ms, TE =13 ms, slide thickness of 3 mm, FOV of 100 mm, matrix of 320×320, and scan duration 2.53 minutes, fat-suppressed T2-weighted (T2FS) with the following parameters: TR =6,170 ms, TE =83 ms, slide thickness of 3 mm, FOV of 100 mm, matrix of 320×320, scan duration 2.59 minutes, and 3-dimensional T2-weighted (3D T2W) sequences were performed for morphological evaluation. The total acquisition time was approximately 18 minutes. No specific preprocessing approach was applied other than distortion correction.

DTI analysis

We performed DTI analysis using Inline Siemens Neuro 3D software (E11 Version, Siemens Healthineers, Munich, Germany). Median nerve fiber tractography was performed from a single voxel seed region of interest (ROI) manually drawn at the center of the median nerve with the reference based on anatomic images. The FA, RD, MD, and AD were extracted from tractography. The number of tracts and mean values of FA, AD, RD, and MD for each tract were retrieved automatically. The following parameters were used for fiber tracking: manual ROI (1 voxel/ROI position), FA threshold 0.20, samples per voxel length 2, step length 1.25 mm, angle threshold 30 degrees, with a Runge-Kutta (fourth-order method) deterministic tractography algorithm (28,29). The FA, AD, RD, and MD values were automatically retrieved from the median nerve passing through the CT at the following 4 focal anatomical sites: the distal radioulnar joint (DRUJ), which is located approximately 3 cm above the distal wrist crease (d), the inlet of the CT at the pisiform level (i), the middle of the CT (m), and the outlet of the CT at the level of the hook of hamate (o). The cross-sectional area (CSA) of the median nerve was measured on T2FS at the tunnel inlet (iCSA). Delta FA and Delta MD represented the differences in FA and MD at the DRUJ and the outlet of the CT, respectively. An example of the median nerve at the DRUJ and CT outlet and reconstructed tractography of the median nerve through the CT in a patient with CTS is shown in *Figure 1*.

Statistical analysis

The mean values of age, body mass index (BMI), FA, AD, RD, and apparent diffusion coefficient (ADC) at 4 anatomical sites along the CT were calculated. Quantitative data were expressed as mean values ± standard deviation (SD). Normality of quantitative data was determined using Kolmogorov–Smirnov tests of normality. The chi-square test (corrected to Fisher's exact test as appropriate), independent-sample *t*-test, and one-way analysis of variance (ANOVA) (or nonparametric tests if nonnormally distributed) were used for group comparisons of DTI parameters and CTS severity. The Pearson coefficient was utilized for assessment of correlations between 2 continuous datasets (DTI parameters with Boston scores, NCS findings, and iCSA). The level of correlation (R-value) was calculated. Univariate linear regression was utilized for calculating beta-coefficients and 95% confidence intervals (CI) of the difference. The receiver operating characteristic (ROC) curve was plotted to calculate the value of DTI parameters in the diagnosis of CTS. The software package SPSS 25.0 (IBM Corp., Armonk, NY, USA) was used for statistical data analysis. A P value <0.05 was considered to indicate statistical significance.

Results

General features

A total of 24 participants (5 males; mean age, 46.3±10.7 years) who met the inclusion criteria were recruited, among whom 15 patients had bilateral disease and 9 patients had unilateral disease. A total of 39 wrists with CTS comprised the study sample. In addition, 10 wrists from healthy volunteers (2 males; mean age, 41.9±10.8 years) were included as the

© Quantitative Imaging in Medicine and Surgery. All rights reserved.

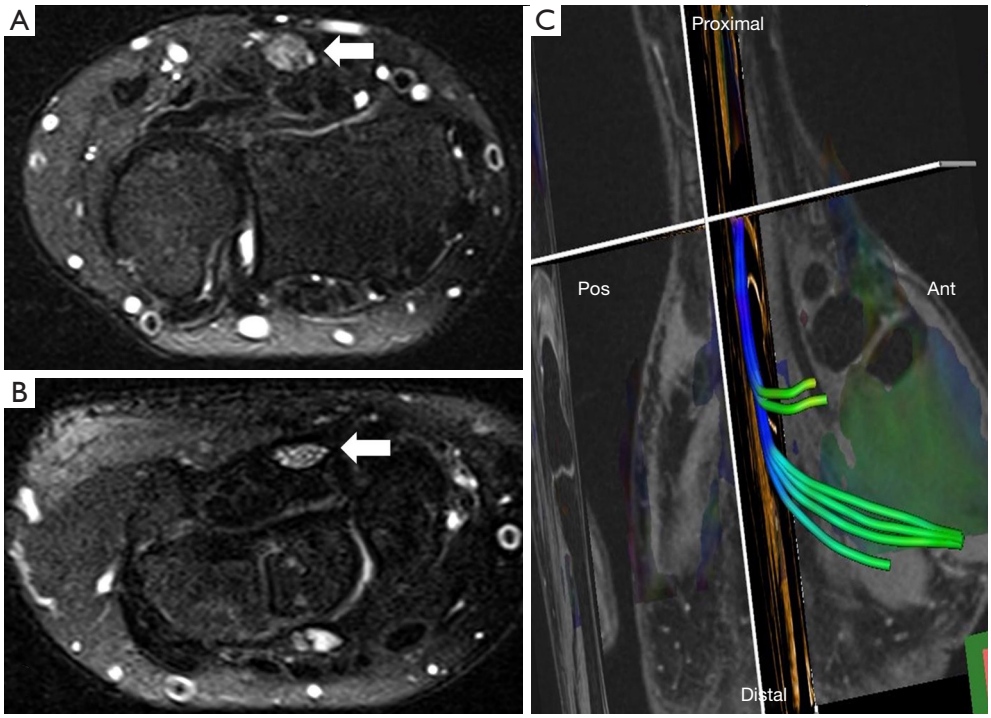

Figure 1 MRI of median nerve at the carpal tunnel. (A) Median nerve (arrow) at the distal radioulnar joint. (B) Median nerve (arrow) at the outlet of the carpal tunnel in a patient with CTS. (A) and (B) axial T2-weighted spectral attenuated inversion recovery. (C) Reconstructed tractography of the median nerve through the carpal tunnel. MRI, magnetic resonance imaging; CTS, carpal tunnel syndrome.

Table 1 Age, BMI, gender, and clinical background of the CTS group and control group

General features	CTS group (n=35)	Control group (n=8)	P
Age (years)	46.3±10.7	41.9±10.8	0.237
BMI (kg/m^2)	23.5±2.6	22.1±1.0	0.202
Female gender [n (%)]	21 (87.5)	4 (66.7)	0.254
Clinical symptom	At least one symptom of CTS (AAEM)	Asymptomatic	1.000

CTS, carpal tunnel syndrome; BMI, body mass index; AAEM, American Association of Electrodiagnostic Medicine.

control group (*Table 1*). There were no cases with missing data during the whole process. There were no significant differences between the CTS group and the control group in gender, age, or BMI.

Clinical and electrophysiology findings

The variables and mean values for the CTS group were as follows: disease duration, 33±23 months; symptom Boston score, 2.6±0.8; function Boston score, 2.1±0.8; distal motor latency time, 4.2±1.2 ms; and sensory conduction velocity, 42.2±14.8 m/s (*Table 2*).

MRI findings

The FA and MD at the outlet of the tunnel (oFA and oMD) of patients and controls are shown as boxplots in *Figure 2*. There was a statistically significant difference between the 2 groups in FA at all 4 abovementioned levels, MD at the DRUJ, inlet and outlet of the CT, AD at the outlet of the CT, and RD at the middle of the CT (P<0.05) (*Table 2*).

FA

Figure 3 shows the correlation between FA at the inlet

© Quantitative Imaging in Medicine and Surgery. All rights reserved.

Table 2 Boston score, distal motor latency, DTI parameters of the patients and control group

DTI parameters	CTS group (mean ± SD)	Control group (mean ± SD)	P value	Mean difference	95% CI (lower, upper)
Symptom Boston score	2.60±0.85	1.00±0.00	<0.001	1.60	1.32, 1.88
Functional Boston score	2.13±0.84	1.00±0.00	<0.001	1.13	0.86, 1.40
dFA	0.46±0.06	0.54±0.07	<0.001	0.09	0.05, 0.13
iFA	0.42±0.05	0.54±0.07	0.001	0.115	0.06, 0.17
mFA	0.41±0.04	0.49±0.04	<0.001	0.07	0.04, 0.10
oFA	0.41±0.05	0.49±0.03	<0.001	0.09	0.05, 0.12
dMD (mm^2/s)	1.34±0.26	1.11±0.24	0.007	0.24	0.07, 0.43
iMD (mm^2/s)	1.46±0.17	1.16±0.37	0.032	0.30	0.03, 0.57
mMD (mm^2/s)	1.47±0.15	1.38±0.12	0.086	0.105	0.01, 0.20
oMD (mm^2/s)	1.49±0.18	1.31±0.19	0.009	0.18	0.03, 0.32
dAD (mm^2/s)	1.81±0.57	2.00±0.68	0.273	-0.19	-0.61, 0.23
iAD (mm^2/s)	2.19±0.33	2.19±0.24	0.922	0.015	–0.21, 0.24
mAD (mm^2/s)	2.38±0.34	2.26±0.26	0.297	0.12	–0.11, 0.35
oAD (mm^2/s)	2.47±0.28	2.19±0.38	0.011	0.585	0.67, 0.50
dRD (mm^2/s)	0.93±0.47	0.69±0.51	0.182	0.23	–0.11, 0.57
iRD (mm^2/s)	1.15±0.26	0.98±0.24	0.075	0.166	–0.017, 0.35
mRD (mm^2/s)	1.21±0.24	0.92±0.08	<0.001	0.285	0.19, 0.38
oRD (mm^2/s)	1.14±0.25	0.83±0.16	<0.001	0.32	0.15, 0.49

CTS, carpal tunnel syndrome; DTI, diffusion tensor imaging; CI, confidence interval; d, i, m, and o, at the distal radioulnar joint, the inlet, the middle, the outlet of the carpal tunnel, respectively; FA, fractional anisotropy; MD, mean diffusivity; RD, radial diffusivity.

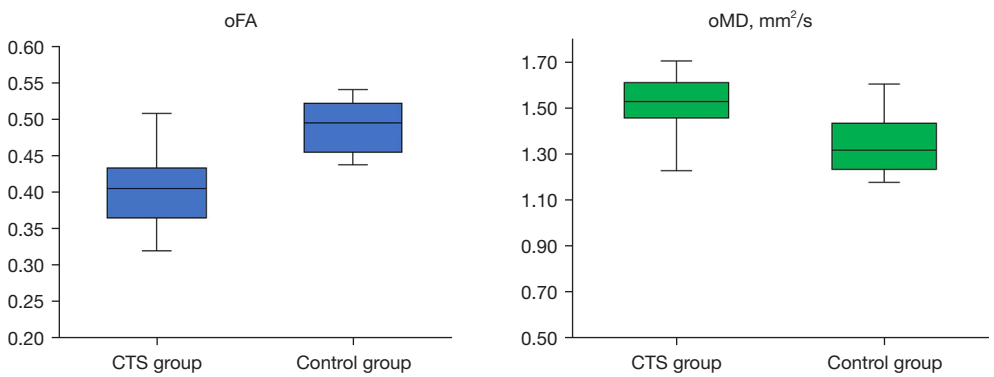

Figure 2 Boxplots of FA value (left) and MD value (right) at the outlet of the carpal tunnel in patients and controls. FA, fractional anisotropy; MD, mean diffusivity; o, outlet of the carpal tunnel.

© Quantitative Imaging in Medicine and Surgery. All rights reserved.

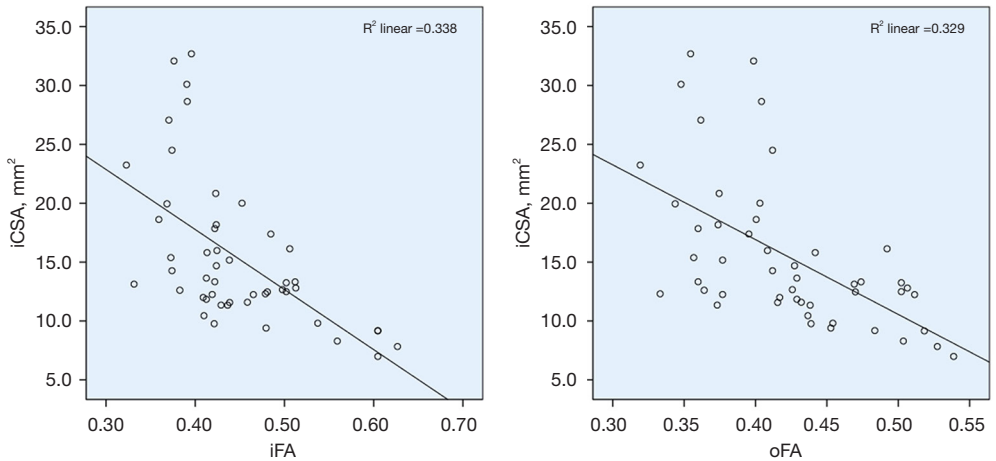

Figure 3 Scatterplots of correlation between FA at the inlet of the carpal tunnel and CSA of the median nerve (left) and correlation between FA at the outlet of the carpal tunnel and CSA of the median nerve (right). FA, fractional anisotropy; CSA, cross-sectional area; i,and o, inlet, and outlet of the carpal tunnel, respectively.

Table 3 Correlations between DTI parameters with Boston scores and electrophysiological parameters

DTI parameters	Symptom Boston score		Function Boston score		Distal motor latency time		iCSA	
	R	P value	R	P value	R	P value	R	P value
iFA	−0.42	0.007	−0.31	0.055	P=0.285		−0.42	0.008
mFA	−0.40	0.012	−0.34	0.032	P=0.995		−0.42	0.006
oFA	−0.40	0.011	−0.37	0.002	P=0.307		−0.45	0.004
dFA								
d, i, m, dMD				P>0.05				
d, i, m, dRD								
d, i, m, dRD								
Delta FA	P=0.36		P=0.26		−0.51	0.01	P=0.448	
Delta MD	P=0.36		P=0.57		0.57	<0.001	P=0.542	

DTI, diffusion tensor imaging; d, i, m, and o, at the distal radioulnar joint, the inlet, the middle, the outlet of the carpal tunnel, respectively; FA, fractional anisotropy; MD, mean diffusivity; RD, radial diffusivity; Delta FA = oFA - dFA; Delta MD = oMD – dMD; iCSA, cross-sectional area at the inlet of the tunnel.

and at the outlet of the CT and CSA of the median nerve. The oFA demonstrated the lowest mean value (0.40±0.05) compared to FA values at the other levels. There was a negative correlation between iCSA and iFA, mFA, and oFA, with oFA showing the strongest negative correlation (R=−0.45, beta-coefficient −0.005, 95% CI: −0.007 to −0.003) (*Tables 3*,*4*). Additionally, oFA and mFA demonstrated a somewhat strong negative correlation with the symptom Boston score and function Boston score (*Table 3*). The oFA demonstrated a correlation with electrophysiological stages (*Table 5*).

MD, RD, and AD

There was no correlation among MD, AD, and RD at all 4 different levels and Boston score, distal motor latency time of the median nerve, and iCSA (*Table 3*). The oMD demonstrated a correlation with electrophysiological stages (*Table 5*).

© Quantitative Imaging in Medicine and Surgery. All rights reserved.

Table 4 The univariate linear regression analysis of factors affecting DTI parameters

DTI parameters	iFA	mFA	oFA	Delta FA	Delta MD
Symptom Boston score					
Beta-coefficient	−0.04	−0.03	−0.04		
P value	<0.001	<0.001	<0.001	0.835	0.595
95% CI (lower, upper)	−0.06, −0.03	−0.04, −0.02	−0.05, −0.02		
Function Boston score					
Beta-coefficient	−0.04	−0.03	−0.04		
P value	<0.001	<0.001	<0.001	0.679	0.785
95% confidence interval (lower, upper)	−0.06, −0.02	−0.05, −0.02	−0.05, −0.02		
Distal motor latency time					
Beta-coefficient				−0.03	0.16
P value	0.142	0.644	0.662	<0.001	<0.001
95% confidence interval (lower, upper)				−0.04, −0.02	0.08, 0.23
iCSA					
Beta-coefficient	−0.007	−0.005	−0.005		
P value	<0.001	<0.001	<0.001	0.49	0.243
95% confidence interval (lower, upper)	−0.009, −0.004	−0.007, −0.003	−0.007, −0.003		

DTI, diffusion tensor imaging; CI, confidence interval; d, i, m, and o, at the distal radioulnar joint, the inlet, the middle, the outlet of the carpal tunnel, respectively; FA, fractional anisotropy; Delta FA = oFA – dFA; Delta MD = oMD – dMD; CSA, cross-sectional area.

Table 5 The relation between DTI parameters with clinical stage and electrophysiological stage

DTI parameters	Electrophysiological stage (P value)	Clinical stage (P value)
dFA	0.35	0.129
d, i, mMD	>0.05	>0.05
d, i, m, oRD	>0.05	>0.05
d, i, m, oAD	>0.05	>0.05
iFA	0.174	0.011
mFA	0.075	0.03
oFA	0.035	0.082
oMD	0.042	0.265
Delta FA	0.504	0.209
Delta MD	0.389	0.186

DTI, diffusion tensor imaging; d, i, m, and o, at the distal radioulnar joint, inlet, middle, and outlet of the carpal tunnel, respectively; FA, fractional anisotropy; MD, mean diffusivity; AD, axial diffusivity; RD, radial diffusivity; DeltaFA = oFA - dFA; DeltaMD = oMD – dMD.

Delta FA and Delta MD

There was a strong positive correlation between Delta MD and distal motor latency time of the median nerve (R=0.57) (*Table 3*, *Figure 4*). There was a strong negative correlation between Delta FA and distal motor latency time of the median nerve (R=–0.51) (*Table 3*, *Figure 4*).

ROC curve analysis

With a cutoff value of 0.45, oFA was the best predictor of a diagnosis of CTS, with a sensitivity of 90%, specificity of 84.6%, and accuracy of 92.1%. It was also shown that dFA and iCSA can be used to increase the sensitivity of the diagnosis (100%, 97.4%) (*Table 6*, *Figure 5*).

Discussion

Main findings

This study aimed to assess the changes of water diffusion within the median nerve in patients with CTS by using

© Quantitative Imaging in Medicine and Surgery. All rights reserved.

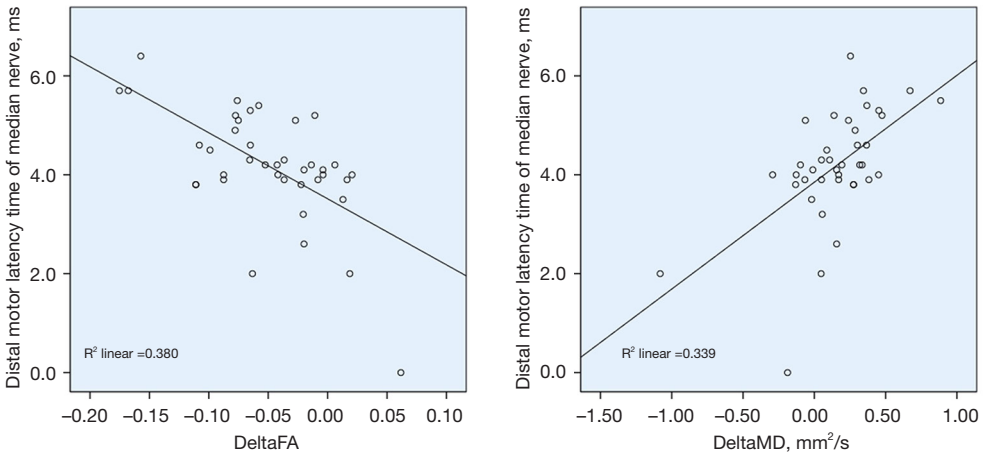

Figure 4 Scatterplots of correlations between Delta FA and distal motor latency time of the median nerve (left) and between Delta MD and distal motor latency time of the median nerve (right). Delta FA = oFA – dFA; Delta MD = oMD – dMD; FA, fractional anisotropy; MD, mean diffusivity; d and o, at the distal radioulnar joint and outlet of the carpal tunnel, respectively.

Table 6 The value of the DTI-derived metrics and iCSA of the median nerve in the diagnosis of CTS

DTI parameters	Cutoff	Sensitivity (%)	Specificity (%)	AUC (%)
dFA	0.46	100	56.4	83.3
iFA	0.46	90	79.5	87.9
mFA	0.43	90	71.8	89.5
oFA	0.45	90	84.6	92.1
dMD (mm^2/s)	1.13	84.6	60	77.4
iMD (mm^2/s)	1.33	71.8	70	74.6
oMD (mm^2/s)	1.43	76.9	80	74.9
oAD (mm^2/s)	2.17	79.5	60	73.6
mRD (mm^2/s)	1.00	79.5	90	86.9
oRD (mm^2/s)	1.00	76.9	90	86.4
iCSA (mm^2)	10.9	97.4	80	95.4

AUC, area under the curve; DTI, diffusion tensor imaging; iCSA, cross-sectional area at the inlet of the tunnel; CTS, carpal tunnel syndrome; d, i, m, and o, at the distal radioulnar joint, inlet, middle, and outlet of the carpal tunnel, respectively; FA, fractional anisotropy; MD, mean diffusivity; AD, axial diffusivity; RD, radial diffusivity.

DTI, and yielded 2 main findings. The first was the correlation of DTI-derived metrics with clinical and electrophysiological parameters. The second was the diagnostic value of different diffusion-derived quantitative parameters in CTS.

Diffusion-derived metrics versus clinical and electrophysiological parameters

The FA expresses the anisotropic diffusion of water molecules within biological tissue (28,30). Within neural structures, water molecules tend to diffuse along the main direction of the white matter tracts or peripheral nerves due to directional axonal structures (31,32). Hence, normal white matter tracts or peripheral nerves usually show high AD. Decreased FA may be caused by damage to the axonal structure or edema (33). Many studies have successfully used diffusion-derived metrics to investigate the effect of brain tumors or other conditions on cerebral white matter tracts (34-37). The DTI method has also been used to investigate CTS (7,10,21,38). In previous studies, the diagnostic ability of DTI was compared to structural parameters or nerve conduction studies; however, the quantitative aspect of diffusion-derived metrics has not been fully investigated. In the current study, the change in diffusion metrics was shown to be correlated with clinical scores and NCS findings. The FA at the CT outlet showed the most significant change among diffusion metrics. Interestingly, there was a negative correlation of oFA with both the symptom and function Boston scores. The oFA was also the best predictor in the diagnosis of CTS. Moreover, oFA was able to distinguish different severity stages. Reduced FA along with increased MD and RD within the CT may be attributed to the edema caused by acute compression. The most significant change was found at the outlet of the CT where the flexor

© Quantitative Imaging in Medicine and Surgery. All rights reserved.

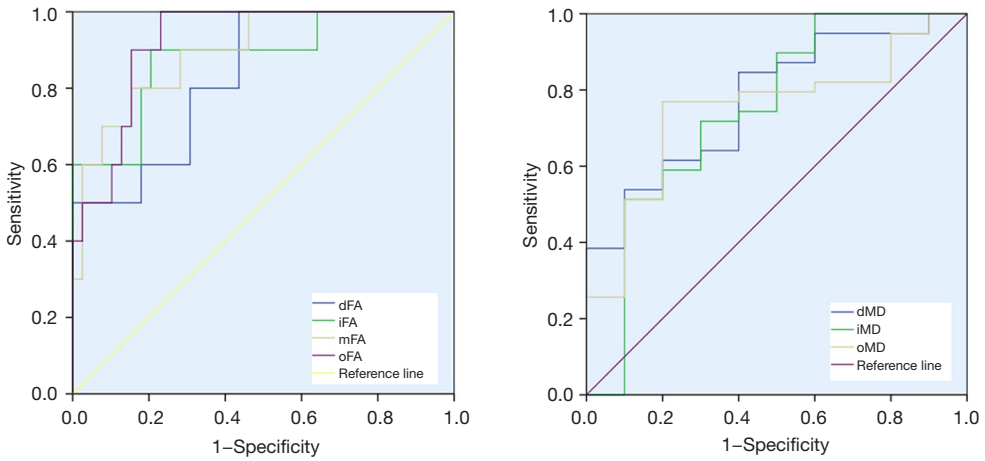

Figure 5 ROC curves and areas under the curve of DTI parameters. ROC, receiver operating characteristic; DTI, diffusion tensor imaging. FA, fractional anisotropy; MD, mean diffusivity; d, i, m, and o, at the distal radioulnar joint, the inlet, the middle, the outlet of the carpal tunnel, respectively.

retinaculum was the thickest, which further supported the argument. Hence, alterations in diffusion metrics may be useful indicators of the compression level. This may set the stage for further studies investigating the potentially added value of diffusion metrics in predicting the clinical severity of CTS, which has implicit prognostic value.

Diagnostic value of diffusion-derived quantitative parameters

Numerous studies have been conducted to investigate the ability of different MRI parameters to diagnose CTS (8,10,21,38). The CSA of the median nerve has been found to be a good diagnostic parameter (38-40) as well as a good indicator for grading CTS (41). Other MRI semiquantitative parameters, such as the flattening ratio of the median nerve, the flexor retinaculum bowing ratio, and the signal intensity ratio of the median nerve compared to that of the hypothenar muscle, have been found to have variable values in the diagnosis and grading of CTS (42-44). The ADC of the median nerve has been found to be of potential value in the diagnosis of CTS (45). Water diffusion has been found to increase proximally (DRUJ) to distally (pisiform) (45). Our findings are in line with previous studies (7,8,10,11,22), in addition to which, we tested different DTI-related metrics at different locations to find out the best discriminators. In our results, oFA was the best predictor of CTS. Our cutoff values of FA at CT are similar to those of other published studies, which range from 0.42 to 0.54 (8-10,22).

To evaluate the severity of compression, in addition to the oFA, we propose to use the new indices 'Delta FA' and 'Delta MD', which reflect alterations in FA and MD when moving proximally (DRUJ) to distally (the outlet of the CT), respectively. Noticeably, Delta FA and Delta MA were found to correlate with the distal motor latency time in NCS. Further studies are needed to explore the potential value of the indices in evaluating CTS.

Limitations and future directions

The main drawbacks of the current study were the limited size of the sample and the cross-sectional study design. A larger sample size with longer observation, especially with postoperative follow-up, is recommended to further explore the potential values of these indices in evaluating CTS. In addition, some patients were scanned bilaterally, and as such the assumptions of independence were violated and the relationship between some variables (*Figure 3*) appeared to be nonlinear, such that the correlation statistics we provided may be misleading.

The alterations of diffusion metrics may provide information regarding the chronicity of the CTS, along with the compression degree. During the acute stage of neural compression, edematous changes within nerves are obvious (22), while chronic compression of the nerve may result in fibrosis (46). Fibrotic changes lead to loss of water content and decrease MD, whilst FA can increase

© Quantitative Imaging in Medicine and Surgery. All rights reserved.

(11,47). Therefore, the pattern of DTI metric change may indicate the chronicity of compression syndrome. This has important implications for the treatment and diagnosis of CTS. Patients with a chronically compressed median nerve may experience delayed symptom relief after standard CT release (48). By contrast, patients receiving early treatment are likely to experience more favorable outcomes (49). Our findings set the stage for future research exploring the potential prognostic value of DTI in CTS and other peripheral nerve compression syndromes.

In conclusion, DTI-derived quantitative metrics potentially add value to the evaluation of CTS. Alterations in the FA of the median nerve along the CT are the most significant feature of CTS and reflect the degree of median nerve compression and clinical deficit. With a cutoff value of 0.45, FA at the carpal outlet has a sensitivity, specificity, and accuracy of 90%, 84.6%, and 92.1% in the diagnosis of CTS, respectively.

Acknowledgments

Funding: This work was supported by Hue University through the Core Research Program (No. NCM. DHH.2020.09).

Footnote

Reporting Checklist: The authors have completed the STROBE reporting checklist. Available at https://qims.amegroups.com/article/view/10.21037/qims-21-910/rc

Conflicts of Interest: All authors have completed the ICMJE uniform disclosure form (available at https://qims.amegroups.com/article/view/10.21037/qims-21-910/coif). The authors have no conflicts of interest to declare.

Ethical Statement: The authors are accountable for all aspects of the work by ensuring that questions related to the accuracy or integrity of any part of the work are appropriately investigated and resolved. The study was conducted in accordance with the Declaration of Helsinki (as revised in 2013). The study was approved by the Ethics Committee of the University of Medicine and Pharmacy, Hue University, Vietnam (No. H2020/159). All patients provided their written informed consent.

Open Access Statement: This is an Open Access article distributed in accordance with the Creative Commons Attribution-NonCommercial-NoDerivs 4.0 International License (CC BY-NC-ND 4.0), which permits the non-commercial replication and distribution of the article with the strict proviso that no changes or edits are made and the original work is properly cited (including links to both the formal publication through the relevant DOI and the license). See: https://creativecommons.org/licenses/by-nc-nd/4.0/.

References

1. Mori S, Zhang J. Principles of diffusion tensor imaging and its applications to basic neuroscience research. Neuron 2006;51:527-39.
2. Kim HJ, Kim SJ, Kim HS, Choi CG, Kim N, Han S, Jang EH, Chung SJ, Lee CS. Alterations of mean diffusivity in brain white matter and deep gray matter in Parkinson's disease. Neurosci Lett 2013;550:64-8.
3. Kubicki M, Westin CF, Maier SE, Mamata H, Frumin M, Ersner-Hershfield H, Kikinis R, Jolesz FA, McCarley R, Shenton ME. Diffusion tensor imaging and its application to neuropsychiatric disorders. Harv Rev Psychiatry 2002;10:324-36.
4. Yoshida S, Oishi K, Faria AV, Mori S. Diffusion tensor imaging of normal brain development. Pediatr Radiol 2013;43:15-27.
5. Leclercq D, Delmaire C, de Champfleur NM, Chiras J, Lehéricy S. Diffusion tractography: methods, validation and applications in patients with neurosurgical lesions. Neurosurg Clin N Am 2011;22:253-68, ix.
6. Kuhn T, Becerra S, Duncan J, Spivak N, Dang BH, Habelhah B, Mahdavi KD, Mamoun M, Whitney M, Pereles FS, Bystritsky A, Jordan SE. Translating state-of-the-art brain magnetic resonance imaging (MRI) techniques into clinical practice: multimodal MRI differentiates dementia subtypes in a traditional clinical setting. Quant Imaging Med Surg 2021;11:4056-73.
7. Wafaie AM, Afifi LM, Moussa KM, Mansour AM, Abbas HM. Role of diffusion tensor imaging in carpal tunnel syndrome: A case control comparative study to electrophysiological tests and clinical assessment. The Egyptian Journal of Radiology and Nuclear Medicine 2018;49:1068-75.
8. Kwon BC, Koh SH, Hwang SY. Optimal parameters and location for diffusion-tensor imaging in the diagnosis of carpal tunnel syndrome: a prospective matched case-control study. AJR Am J Roentgenol 2015;204:1248-54.
9. Wang CK, Jou IM, Huang HW, Chen PY, Tsai HM, Liu YS, Lin CC. Carpal tunnel syndrome assessed

© Quantitative Imaging in Medicine and Surgery. All rights reserved.

with diffusion tensor imaging: comparison with electrophysiological studies of patients and healthy volunteers. Eur J Radiol 2012;81:3378-83.
10. Wang H, Ma J, Zhao L, Wang Y, Jia X. Utility of MRI Diffusion Tensor Imaging in Carpal Tunnel Syndrome: A Meta-Analysis. Med Sci Monit 2016;22:736-42.
11. Wu W, Niu Y, Kong X, Liu D, Long X, Shu S, Su X, Wang B, Liu X, Ma Y, Wang L. Application of diffusion tensor imaging in quantitatively monitoring chronic constriction injury of rabbit sciatic nerves: correlation with histological and functional changes. Br J Radiol 2018;91:20170414.
12. Padua L, Coraci D, Erra C, Pazzaglia C, Paolasso I, Loreti C, Caliandro P, Hobson-Webb LD. Carpal tunnel syndrome: clinical features, diagnosis, and management. Lancet Neurol 2016;15:1273-84.
13. Wahab KW, Sanya EO, Adebayo PB, Babalola MO, Ibraheem HG. Carpal Tunnel Syndrome and Other Entrapment Neuropathies. Oman Med J 2017;32:449-54.
14. Atroshi I, Gummesson C, Johnsson R, Ornstein E, Ranstam J, Rosén I. Prevalence of carpal tunnel syndrome in a general population. JAMA 1999;282:153-8.
15. Wilder-Smith EP, Seet RC, Lim EC. Diagnosing carpal tunnel syndrome--clinical criteria and ancillary tests. Nat Clin Pract Neurol 2006;2:366-74.
16. Vo NQ, Nguyen THD, Nguyen DD, Le TB, Le NTN, Nguyen TT. The value of sonographic quantitative parameters in the diagnosis of carpal tunnel syndrome in the Vietnamese population. J Int Med Res 2021;49:3000605211064408.
17. Kumari A, Singh S, Garg A, Prakash A, Sural S. Tingling hand: magnetic resonance imaging of median nerve pathologies within the carpal tunnel. Pol J Radiol 2019;84:e484-90.
18. Peer S, Gruber H, Loizides A. Sonography of carpal tunnel syndrome: why, when and how. Imaging Med 2012;4:287-97.
19. Martín Noguerol T, Barousse R, Socolovsky M, Luna A. Quantitative magnetic resonance (MR) neurography for evaluation of peripheral nerves and plexus injuries. Quant Imaging Med Surg 2017;7:398-421.
20. Heckel A, Weiler M, Xia A, Ruetters M, Pham M, Bendszus M, Heiland S, Baeumer P. Peripheral Nerve Diffusion Tensor Imaging: Assessment of Axon and Myelin Sheath Integrity. PLoS One 2015;10:e0130833.
21. Stein D, Neufeld A, Pasternak O, Graif M, Patish H, Schwimmer E, Ziv E, Assaf Y. Diffusion tensor imaging of the median nerve in healthy and carpal tunnel syndrome subjects. J Magn Reson Imaging 2009;29:657-62.
22. Rojoa D, Raheman F, Rassam J, Wade RG. Meta-analysis of the normal diffusion tensor imaging values of the median nerve and how they change in carpal tunnel syndrome. Sci Rep 2021;11:20935.
23. von Elm E, Altman DG, Egger M, Pocock SJ, Gøtzsche PC, Vandenbroucke JP; STROBE Initiative. The Strengthening the Reporting of Observational Studies in Epidemiology (STROBE) statement: guidelines for reporting observational studies. Ann Intern Med 2007;147:573-7.
24. American Association of Electrodiagnostic Medicine, American Academy of Neurology, and American Academy of Physical Medicine and Rehabilitation. Practice parameter for electrodiagnostic studies in carpal tunnel syndrome: summary statement. Muscle Nerve 2002;25:918-22.
25. Practice parameter for carpal tunnel syndrome (summary statement). Report of the Quality Standards Subcommittee of the American Academy of Neurology. Neurology 1993;43:2406-9.
26. Levine DW, Simmons BP, Koris MJ, Daltroy LH, Hohl GG, Fossel AH, Katz JN. A self-administered questionnaire for the assessment of severity of symptoms and functional status in carpal tunnel syndrome. J Bone Joint Surg Am 1993;75:1585-92.
27. Stevens JC, Sun S, Beard CM, O'Fallon WM, Kurland LT. Carpal tunnel syndrome in Rochester, Minnesota, 1961 to 1980. Neurology 1988;38:134-8.
28. Basser PJ, Pajevic S, Pierpaoli C, Duda J, Aldroubi A. In vivo fiber tractography using DT-MRI data. Magn Reson Med 2000;44:625-32.
29. Conturo TE, Lori NF, Cull TS, Akbudak E, Snyder AZ, Shimony JS, McKinstry RC, Burton H, Raichle ME. Tracking neuronal fiber pathways in the living human brain. Proc Natl Acad Sci U S A 1999;96:10422-7.
30. Basser PJ, Mattiello J, LeBihan D. MR diffusion tensor spectroscopy and imaging. Biophys J 1994;66:259-67.
31. Mori S, Crain BJ, Chacko VP, van Zijl PC. Three-dimensional tracking of axonal projections in the brain by magnetic resonance imaging. Ann Neurol 1999;45:265-9.
32. Pierpaoli C, Jezzard P, Basser PJ, Barnett A, Di Chiro G. Diffusion tensor MR imaging of the human brain. Radiology 1996;201:637-48.
33. Aung WY, Mar S, Benzinger TL. Diffusion tensor MRI as a biomarker in axonal and myelin damage. Imaging Med 2013;5:427-40.
34. Nguyen-Thanh T, Reisert M, Anastasopoulos C, Hamzei

© Quantitative Imaging in Medicine and Surgery. All rights reserved.

F, Reithmeier T, Vry MS, Kiselev VG, Weyerbrock A, Mader I. Global tracking in human gliomas: a comparison with established tracking methods. Clin Neuroradiol 2013;23:263-75.
35. Anastasopoulos C, Reisert M, Kiselev VG, Nguyen-Thanh T, Schulze-Bonhage A, Zentner J, Mader I. Local and global fiber tractography in patients with epilepsy. AJNR Am J Neuroradiol 2014;35:291-6.
36. Higano S, Zhong J, Shrier DA, Shibata DK, Takase Y, Wang H, Numaguchi Y. Diffusion anisotropy of the internal capsule and the corona radiata in association with stroke and tumors as measured by diffusion-weighted MR imaging. AJNR Am J Neuroradiol 2001;22:456-63.
37. Maier SE, Sun Y, Mulkern RV. Diffusion imaging of brain tumors. NMR Biomed 2010;23:849-64.
38. Koh SH, Kwon BC, Park C, Hwang SY, Lee JW, Kim SS. A comparison of the performance of anatomical MRI and DTI in diagnosing carpal tunnel syndrome. Eur J Radiol 2014;83:2065-73.
39. Ng AWH, Griffith JF, Tong CSL, Law EKC, Tse WL, Wong CWY, Ho PC. MRI criteria for diagnosis and predicting severity of carpal tunnel syndrome. Skeletal Radiol 2020;49:397-405.
40. Kasundra GM, Sood I, Bhargava AN, Bhushan B, Rana K, Jangid H, Shubhkaran K, Pujar GS. Carpal tunnel syndrome: Analyzing efficacy and utility of clinical tests and various diagnostic modalities. J Neurosci Rural Pract 2015;6:504-10.
41. Bagga B, Sinha A, Khandelwal N, Modi M, Ahuja CK, Sharma R. Comparison of Magnetic Resonance Imaging and Ultrasonography in Diagnosing and Grading Carpal Tunnel Syndrome: A Prospective Study. Curr Probl Diagn Radiol 2020;49:102-15.
42. Uchiyama S, Itsubo T, Yasutomi T, Nakagawa H, Kamimura M, Kato H. Quantitative MRI of the wrist and nerve conduction studies in patients with idiopathic carpal tunnel syndrome. J Neurol Neurosurg Psychiatry 2005;76:1103-8.
43. Bendszus M, Koltzenburg M, Wessig C, Solymosi L. Sequential MR imaging of denervated muscle: experimental study. AJNR Am J Neuroradiol 2002;23:1427-31.
44. Dong Q, Jacobson JA, Jamadar DA, Gandikota G, Brandon C, Morag Y, Fessell DP, Kim SM. Entrapment neuropathies in the upper and lower limbs: anatomy and MRI features. Radiol Res Pract 2012;2012:230679.
45. Allam MFAB, Ibrahiem MA, Allam AFAB. The value of quantitative MRI using 1.5T magnet in diagnosis of carpal tunnel syndrome. The Egyptian Journal of Radiology and Nuclear Medicine 2017;48:201-6.
46. Li Q, Chen J, Chen Y, Cong X, Chen Z. Chronic sciatic nerve compression induces fibrosis in dorsal root ganglia. Mol Med Rep 2016;13:2393-400.
47. Lindberg PG, Feydy A, Le Viet D, Maier MA, Drapé JL. Diffusion tensor imaging of the median nerve in recurrent carpal tunnel syndrome - initial experience. Eur Radiol 2013;23:3115-23.
48. Masud M, Rashid M, Malik SA, Ibrahim Khan M, Sarwar SU. Does the Duration and Severity of Symptoms Have an Impact on Relief of Symptoms after Carpal Tunnel Release? J Brachial Plex Peripher Nerve Inj 2019;14:e1-8.
49. Chandra PS, Singh PK, Goyal V, Chauhan AK, Thakkur N, Tripathi M. Early versus delayed endoscopic surgery for carpal tunnel syndrome: prospective randomized study. World Neurosurg 2013;79:767-72.

Cite this article as: Vo NQ, Hoang NT, Nguyen DD, Nguyen THD, Le TB, Le NTN, Nguyen TT. Quantitative parameters of diffusion tensor imaging in the evaluation of carpal tunnel syndrome. Quant Imaging Med Surg 2022;12(6):3379-3390. doi: 10.21037/qims-21-910

© Quantitative Imaging in Medicine and Surgery. All rights reserved.